

Ensemble reconstruction of the atmospheric column from surface pressure using analogues

Pascal Yiou · Tamara Salameh · Philippe Drobinski · Laurent Menut · Robert Vautard · Mathieu Vrac

Received: 1 June 2012 / Accepted: 5 December 2012 / Published online: 18 December 2012
© Springer-Verlag Berlin Heidelberg 2012

Abstract We present a statistical method to reconstruct continuous atmospheric fields on various pressure levels, given a constraint at the surface. The method is based on analogues of circulation and taking into consideration the time sequence of the analogues. The method is tested on the 2001–2011 period, with an emphasis on the year 2010. We base the atmospheric reconstruction on reanalysis data from 1948 to 2000, and use a constraint of sea-level pressure for 2001–2011. The pattern correlation scores appear to be significant most of the time, although score flaws are occasionally detected. Those flaws are mainly due to the time continuity constraint that is imposed on the reconstruction, which lowers the possibility of finding matching analogues. This method offers an ensemble of atmospheric reconstructions, and presents a computationally cheap alternative to data assimilation for a climate model, although with lower scores.

Keywords Circulation analogues · Climate reconstructions · North Atlantic variability

1 Introduction and motivation

Reconstructions of sea-level pressure above the North Atlantic for the past centuries have been available from historical meteorological observations (Ansell et al. 2006;

Luterbacher et al. 2000), sometimes on daily time scales. Such reconstructions are based on pressure observations from continental meteorological stations. Some reconstructions have been interpolated on regular grid cells, which makes them easier to compare with contemporary re-analyses (Kalnay et al. 1996; Uppala et al. 2005). Initiatives to build a global atmospheric re-analysis of the climate of last centuries have emerged in order to reconstruct variations of the three dimensional atmospheric field. Those initiatives used assimilation methods to constrain a state-of-the-art climate model with ancient meteorological observations (Compo et al. 2006; Gong et al. 2007; Widmann et al. 2010; Compo et al. 2011). The downside of those re-analysis projects is their spatial resolution, which has been limited to 2–3°, for obvious computational reasons and the scarcity of observations on a global scale.

This work is motivated by the study of meteorological events of the last millennium that are regional by essence, like heatwaves (Vautard et al. 2007; Zampieri et al. 2009), cold spells or investigate the impacts of volcanic eruptions on air quality (Chenet et al. 2005; Schmidt et al. 2011). Regional climate models yield the relevant horizontal resolution to investigate such events (Seneviratne et al. 2006; Fischer et al. 2007; Zampieri et al. 2009). Their use for a study of historical events is limited by the availability of three dimensional initial and boundary conditions, especially for pressure, temperature and humidity fields. The historical meteorological records are mainly available on one vertical level, namely at the surface, which is a priori not sufficient to force a regional climate model. Thus, there is a need of methodologies to reconstruct the vertical structure of fields like geopotential heights or temperature, given surface observations. One path has been the assimilation of pressure observations in an atmospheric

P. Yiou (✉) · T. Salameh · R. Vautard · M. Vrac
Laboratoire des Sciences du Climat et de l'Environnement,
UMR CEA-CNRS-UVSQ, Gif-sur-Yvette, France
e-mail: pascal.yiou@lscce.ipsl.fr

P. Drobinski · L. Menut
Laboratoire de Météorologie Dynamique,
UMR CNRS-UPMC-ENS-X, Palaiseau, France

general circulation model in order to provide a long-term climate re-analysis (e.g. Compo et al. 2006).

The goal of this work is to develop an alternative statistical method allowing the reconstruction of an ensemble 3D field of geopotential heights and surface temperature that is consistent with surface observations. We propose a method that is based on analogues of atmospheric patterns obtained from a modern re-analysis dataset. This method has been recently used for case studies and trend estimates for European climate variables (Yiou et al. 2007; Vautard and Yiou 2009; Cattiaux et al. 2010). Hence, rather than running a numerical weather prediction model and assimilating observations, we use reanalysis data that are analogous to surface observations, with a constraint on time continuity. The region of focus is the North Atlantic. We base our analysis on NCEP reanalyses (Kalnay et al. 1996).

We tested our methodology on the decade from 2001 to 2011, with an emphasis on year 2010. The main motivation for this choice was that an Icelandic volcanic eruption occurred in Spring 2010. This volcanic eruption disrupted aviation activities during a whole month. Therefore the year 2010 is (for fortuitous reasons) an interesting period to test a circulation reconstruction. We reconstruct the three dimensional atmospheric circulation in 2001–2011, from sea-level pressure data and re-analysed geopotential heights between 1948 and 2000. The method is also tested for surface temperature. This paper is a preliminary methodological step to obtain an ensemble of historical regional climate simulations.

The methodology is detailed in Sect. 2. The data we use and the choice of the parameters are given in Sect. 3. The application to the 2001–2011 decade is illustrated in Sect. 4. Discussion and conclusions are drawn in Sect. 5.

2 Methodology

We want to reconstruct a three-dimensional atmospheric flow field \mathbf{Z} for geopotential heights at various pressure levels, sea-level pressure and surface air temperature. We assume that a “target” dataset \mathcal{T} of predictors \mathbf{X} is available for a given period of time. Mathematically, the goal is to build an estimate $\hat{\mathbf{Z}}$ of \mathbf{Z} given an observation of its *trace* \mathbf{X} at a boundary. Loosely speaking, if a partial differential equation is defined on a given domain, the *trace operator* is a restriction of the equation to the boundary of the domain. Here we will consider that \mathbf{X} is a daily field of sea-level pressure (SLP) anomalies with respect to the seasonal cycle. Here, we want to estimate geopotential heights at various pressure levels and surface temperature that are consistent with the available two-dimensional SLP field. We hence focus on the reconstruction of

geopotential height anomalies at 1,000, 850, 500 and 300 mb (respectively z1000, z850, z500 and z300) and surface temperature.

We assume that a reference database \mathcal{R} of three-dimensional atmospheric flow field \mathbf{Z} (including the variable \mathbf{X}) is available for a sufficiently long period to sample the range of \mathbf{X} .

The first step of our approach is to find analogues of \mathbf{X} from the dataset \mathcal{T} , in the reference database \mathcal{R} . \mathcal{T} and \mathcal{R} could stem from two different re-analysis or model simulation data sets or distant time periods.

For a given field $X_i^{(T)}$ in the target dataset \mathcal{T} , we find a day t_i in the reference database \mathcal{R} that optimizes a distance or a correlation (linear or rank) with $X_i^{(T)}$. For a (Euclidean) distance, this corresponds to:

$$t_i = \arg \min_{j \in \mathcal{R}} d(X_i^{(T)}, X_j^{(R)}). \quad (1)$$

The K “best” analogues (e.g., $K = 10$ here) are the sorted optima of distance or correlation. The estimates $\hat{\mathbf{Z}}_i^{(T)}$ are obtained from $\mathbf{Z}_{t_i}^{(R)}$. This method of analogues has been used in various downscaling studies (Yiou et al. 2007; Vautard and Yiou 2009; Zorita and von Storch 1999) to determine the contribution of the atmospheric circulation on surface temperature. The caveat of this simple approach is that a sequence of consecutive days might not yield consecutive dates of best analogues. This potentially hinders the time continuity and differentiability of analogues at other pressure levels.

In order to achieve time differentiability (or at least continuity), we consider moving “windows” $W_i^{(T)}$ of N consecutive days (e.g. $N = 6$) in the dataset \mathcal{T} :

$$W_i^{(T)} = \left(X_i^{(T)}, \dots, X_{i+N-1}^{(T)} \right). \quad (2)$$

We then seek analogues of $W_i^{(T)}$ in \mathcal{R}^N . This constrains the analogues to yield consecutive days, which implies an ad hoc time differentiability. This is based on the assumption that continuity is achieved from one day to the next. The rationale for imposing differentiability and continuity is to constrain the variability on all pressure levels. For a given day, SLP might not constrain upper level atmospheric variability, but a sequence of SLP patterns is more likely to. We loosely justify this claim by the “embedding” theorem for dynamical systems (Mañé 1981; Takens 1981). If we assume that the atmospheric motion can be described by a multivariate dynamical system whose dimension is M , and one of the dimensions is carried by SLP variations, then, a sequence of “delayed” SLP vectors can generically reconstruct the M dimensional dynamics of the full attractor, provided the size of the delayed vectors is large enough. This theorem was the

basis for many time series analysis methodological developments (Vautard et al. 1992; Ghil et al. 2002). We emphasize that the embedding theorem necessitates the validation of quite a few hypotheses that we cannot verify here, but it heuristically sets the rationale for our choice of computing analogues on time “windows” of a climate variable.

The methodology proceeds in three steps:

1. Determination of analogue dates in a database \mathcal{R} , for moving windows in the target dataset \mathcal{T} ,
2. Computation of time varying weights (proportional to the distance of the estimated date to the window center) in the reference database \mathcal{R} in order to ensure continuous transitions between moving windows,
3. Computation of analogues for all variables (at other pressure levels or temperature), from dates and weights in the reference database \mathcal{R} .

We first search for windows of consecutive days in the database \mathcal{R} that optimize the distance (or the correlation) with the target moving window in \mathcal{T} . This corresponds to:

$$t_i = \arg \min_{j \in \mathcal{R}} d(W_i^{(T)}, W_j^{(R)}) \tag{3}$$

for a (Euclidean) distance. By construction, each $W_j^{(R)}$ preserves the piecewise differentiability in time (i.e. for each window of size N) of the estimates $\hat{W}_i^{(T)} = W_{t_i}^{(R)}$.

The windows in the dataset \mathcal{T} can be moved by increments of δ (e.g., $\delta = N/2$), so that, if \mathcal{T} covers a whole year, $365/\delta$ analogues of N consecutive days are computed. A trade-off between a smooth reconstruction and its variability is obtained with the increment parameter $\delta = N/2$. If δ is small compared to N , then the averaging procedure lowers the variance of the reconstruction, while large δ can produce discontinuities.

Once the dates of K best analogues of N -day windows are computed, the overall field reconstruction for each day t in \mathcal{T} is made by averaging the moving windows overlapping t . The reconstruction procedure can be applied for the K best analogues, hence providing K reconstructions. For example, considering the first analogues, if time $t \in \mathcal{T}$ belongs to two windows, $W_i^{(T)}$ and $W_{i'}^{(T)}$, the reconstruction at t \hat{X}_t will be an average of the analogues of those two windows in \mathcal{R} , weighed by the proximity of t to the centers of $W_i^{(T)}$ and $W_{i'}^{(T)}$. If t is the k th element in $[i, i + N - 1]$ and the k' th element in $[i', i' + N - 1]$, then:

$$\hat{X}_t = \alpha_1 X_k^{(T)} + \alpha_2 X_{k'}^{(T)} \tag{4}$$

where the weights α_n are proportional to $k - i$ and $k' - i'$ and sum to 1. If the windows are shifted by increments of $\delta < N/2$, more than two windows can include a given time t . In such a case, the averaging and weighing is done in the same fashion. This procedure is illustrated in Fig. 1.

The weights ensure that the overlapping window procedure yields an overall time continuity and differentiability (which depends on the weight choice), because the sequence in each $W_i^{(R)}$ is composed of observed consecutive days. We note that the averaging procedure necessarily produces a reconstruction with a lower variance than the estimated field. The reduction of variance is proportional to the number of overlapping windows covering each time increment. The weights themselves do not depend on the analogue order (first or K th). Therefore the same averaging procedure is done on all other analogues.

Hence, in principle, this method provides an ensemble of K atmospheric reconstructions that are optimally coherent (in the sense of the metric that is used) with a target dataset \mathcal{T} with a constraint at one boundary. This ensemble can be expanded by mixing local windows of different analogue order: for instance, the reconstruction in Eq. (4) could combine the first analogue for the k th element and the second analogue for the k' th.

The quality of the reconstruction can be tested with the Euclidean distance (or RMS) and spatial rank correlation. The RMS shows the overall proximity of maps in terms of means and variances. The rationale for using rank correlation is that it favors structures and is less sensitive to large deviations. Hence correlation is not sensitive to global averages or variances, and mostly accounts for the similarity of patterns. For example, two maps with very different baselines (and large RMS value) could yield similar patterns (and large correlations).

In our study, the RMS and rank correlation scores are computed for every day of the dataset \mathcal{T} , and for all reconstructed variables (anomalies of SLP, z1000, z850, z500, z300 and surface air temperature). In this study, for each day t in \mathcal{T} , the analogues are sought in all days in \mathcal{R} . Imposing a search within 30 calendar days of t does not

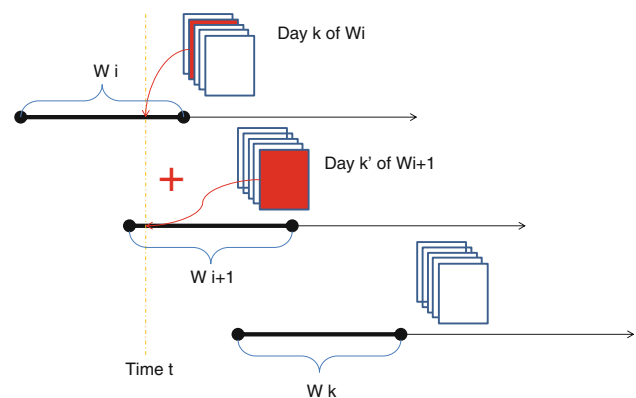


Fig. 1 Schematic of the analogue choice and weighing. For a given time t and a given analogue $a \in \{1, \dots, K\}$, the reconstructed field \hat{X}_t is the average of the windows $W_i^{(R)}$ that include t . The maps at time t in the windows $W_i^{(R)}$ are shown in red

change significantly the results, because the anomalies also have a seasonal cycle in the variance.

3 Data and parameters

The target dataset \mathcal{T} is composed of pressure related atmospheric variables (SLP, z1000, z850, z500 and z300) and surface air temperature in 2010. The predictor variable that we use is SLP anomalies in 2001–2011, and we want to reconstruct all other fields during that period. The daily anomalies were computed relative to 1961–1990 daily means for all the atmospheric fields.

The reference dataset \mathcal{R} is based on the period between 1948 and 2000. For simplicity, we chose a single database for \mathcal{T} and \mathcal{R} , namely the NCEP re-analysis (Kalnay et al. 1996). The method is sufficiently flexible so that \mathcal{T} can cover a period of time in a given database, and \mathcal{R} be taken from another database (e.g. another reanalysis dataset or a long control simulation from a climate model). In any case, the datasets must have the same resolution (or be interpolated on the same spatial grid). We will not test this possibility in this paper and focus on the results of a straightforward application.

We considered the North Atlantic region (80W–35E; 25–70N), for which other analyses of circulation analogues

have been performed. We took daily averages from those atmospheric fields.

We chose a fixed window size of $N = 6$ days for the North Atlantic region. This is motivated by imposing synoptic situations to last at least 5 days (Kimoto and Ghil 1993; Michelangeli et al. 1995), especially in the winter. In the summer, this choice could be revised, with a smaller window size (e.g. $N = 2$). In such a case, the relation with an underlying dynamical structure is jeopardized because the embedding theorem does not apply. We note that other distances can be applied, or one could maximize a correlation. We use the Euclidean distance (or root mean square, RMS) to be coherent with previous studies.

We took a shifting increments δ of 3 days. In this way, each day in 2001–2011 is covered by two sliding analogue windows.

4 Results

The evolution of the RMS and correlation values between the reconstructed and “observed” fields are shown in Fig. 2 for the first analogue in year 2010. For comparison purposes between variables, the RMS values are normalized by the standard deviation in all subsequent figures.

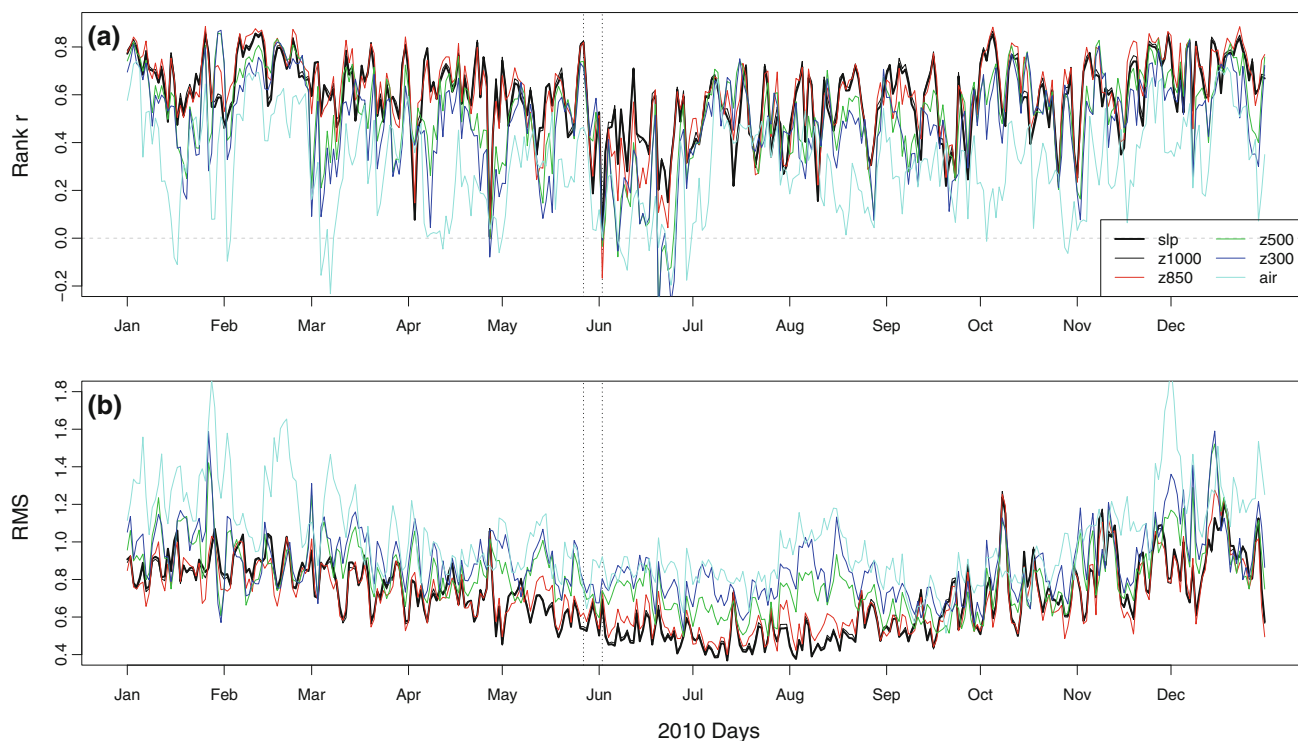
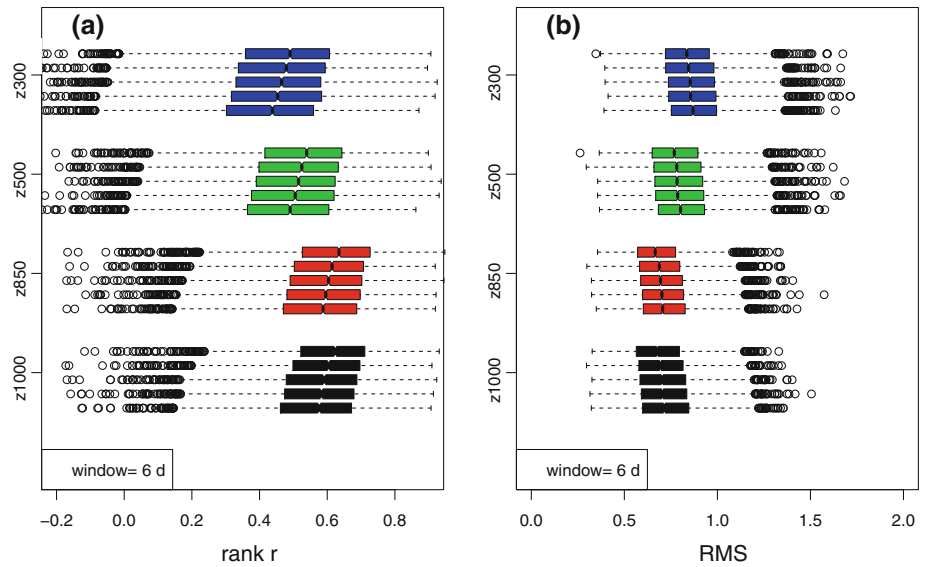


Fig. 2 Skill of the first analogues with windows of size $N = 6$ days and increments of $\delta = 3$ days in 2010 for NCEP re-analysis. **a** Evolution of rank correlation between analogue reconstructions and re-analysis fields at various heights. **b** RMS between analogue

reconstructions and NCEP re-analysis fields. The RMS values are normalized by the SD at each pressure level. The vertical dashed lines indicate May 27th and June 2nd 2010

Fig. 3 Global correlation and RMS values for a window size of $N = 6$ days and shifts of $\delta = 3$ days in 2001–2011 for NCEP re-analysis for geopotential height anomalies. The RMS is normalized by the standard deviation. The *box-and-whisker plots* show the distribution of scores for the first five analogues (from *top* to *bottom*)



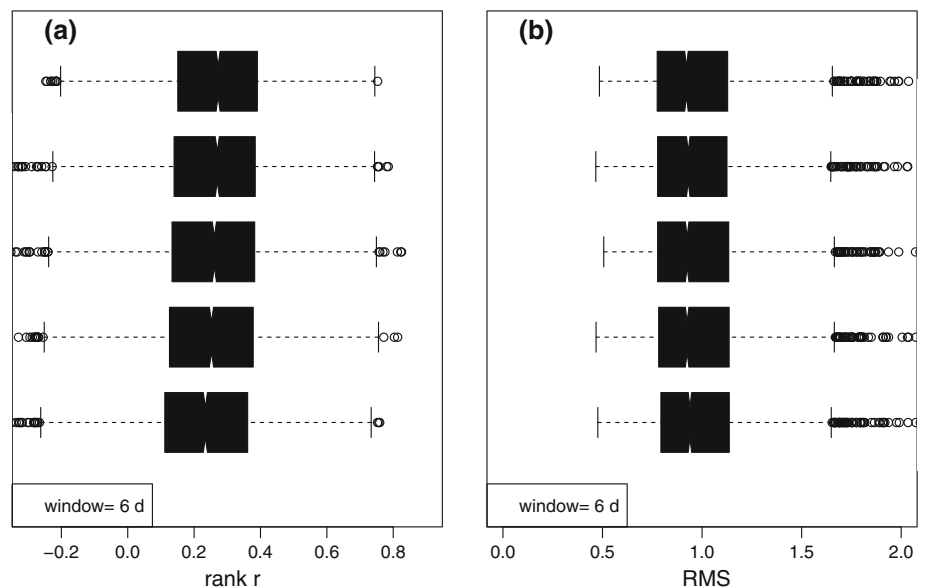
The rank correlation skill for SLP ranges between 0 and 0.89, with 80 % of the values between 0.39 and 0.79. The values of the correlation scores are not significantly degraded when geopotential fields far from the surface are evaluated. The RMS values for geopotential fields are proportional to pressure height, which is expected because the variance of the atmospheric fields increase with altitude. Thus, the RMS values were normalized by the spatial standard deviation for each geopotential height in Fig. 2. The correlation and RMS values for surface temperature are lower than for pressure or geopotential heights, although the correlation is generally significantly positive.

We note that the correlation scores can reach low values (and even occasionally negative during ≈ 10 days) for

geopotential heights higher than $z500$. We interpret this lack of skill by the fact that no proper analogue of $N = 6$ day windows (in 2010) could be found for those days in the dataset between 1948 and 2000. If we change the window length to $N = 2$ (and shifts every $\delta = 1$ day), the skill is improved (not shown), with correlations all above 0.4 for SLP. In this case, the correlation between reanalysis data and reconstruction for $z300$ reaches a negative value once. Although the correlation score is generally higher when N is smaller, the spread of the scores (for all geopotential levels) increases, suggesting a loss of temporal coherence along the vertical due to a weaker time constraint.

We verify the reconstruction skill of the other analogues for geopotential heights in Fig. 3 for the period 2001–2011.

Fig. 4 Global correlation and RMS values for a window size of $N = 6$ days and shifts of $\delta = 3$ days in 2001–2011 for NCEP re-analysis for surface air temperature. The RMS is normalized by the SD. The *box-and-whisker plots* show the distribution of scores for the first five analogues (from *top* to *bottom*)



The correlation scores are barely altered by higher order analogues, although, by construction, the RMS values (slightly) decrease with the order of the analogue. The reconstruction scores for surface air temperature is shown in Fig. 4. Although the correlation and RMS values are lower than for geopotential heights, the order of the analogues does not induce a major degradation of the reconstruction.

We find a seasonality in the analogue scores for all variables (Fig. 5). Generally the correlation scores are higher in the winter and lower in the spring, while the RMS values are higher in summer and lower in winter and fall (the RMS score is “better” or “higher” when the distance value is small). Thus we find an apparent anticorrelation between the two types of scores.

The explanation of the seasonality in RMS values lies in the increase of spatial variance of pressure patterns in the winter, which naturally increases the RMS values. The spatial variance of atmospheric fields is lower in the summer, which implies that the RMS has lower values.

The weak seasonality in correlation, with higher values in winter, is explained by the stronger baroclinicity of the flow in the winter and hence larger variance. For example, the North Atlantic winter atmospheric circulation is well described by four weather regimes (Michelangeli et al. 1995), with a high index of classifiability, implying that the correlation of the pressure patterns within each regime is high. This means that if the analogues of pressure are in the same weather regime as the target field then they necessarily have a good correlation. Low scores can be due to the difficulty to reproduce an unusual sequence of weather regimes, or unusual patterns. Even though weather regimes can last for a few days, their transitions yield preferred paths, so that some sequences are less frequent than others (Kondrashov et al. 2004). Conversely, North Atlantic summer circulation has a low index of classifiability due to a more barotropic flow (Michelangeli et al. 1995). This implies that, although RMS yields low values, the patterns have low correlations because the classes of circulation are not clearly distinguished. In practice, it is useful to reduce the window length in order to investigate the cause of the poor correlation performance (unusual pattern or unusual sequence of patterns).

We selected two days in May–June 2010 with high and low correlation score in SLP reconstruction (Fig. 2) to illustrate the performance of the method on high and low scores. The day with the lowest score in SLP is reached on June 2nd 2010 ($r = 0$) and the highest score is May 27th 2010 ($r = 0.82$). The choice of the season was motivated by the timing of the Icelandic volcanic eruptions in 2010. In order to avoid a tedious redundancy, we only show results

for the evolution of SLP, z500 and z300 over three day windows.

Around June 2nd, the SLP yields an Atlantic low pattern, and shows a pressure high over Scandinavia (Fig. 6). Between June 1st and 3rd, the high pressure zone shifts westward to the Great Britain, while the Atlantic low stays stable. The first analogue also yields an Atlantic low, but the high pressure zone is shifted to the north west. The z500 and z300 features are qualitatively similar, albeit with smoothed features in the analogue reconstruction. In particular, the local low over the Balkans is missed in the reconstruction. The observed temperature patterns show warm anomalies over the Labrador, Southern Greenland, Spain and central Europe (Fig. 7). Negative anomalies are observed in France. The analogue reconstruction reproduces the warm anomalies over the Labrador, Greenland and Spain. The warm central European anomaly has a shifted and weaker amplitude. The cold anomaly over France seems missed during June 2nd 2010. This is connected to the different pressure structures captured by the pressure and lower level geopotential height analogues on that day. An analysis with a smaller window size ($N = 2$) increases to positive the analogue scores for SLP during those dates (not shown). This suggests that the observed sequence of patterns is rather unusual.

The pressure structure around May 27th yields a more pronounced Atlantic low structure, with a positive pressure anomaly over southern Greenland (Figs. 8, 9). The first analogue reconstructions cannot pick the observed dynamical feature, with a weakening of the positive anomaly over southern Greenland, and a strengthening of the low over the North Atlantic. Instead, it shows an eastward shift of the Arctic positive anomaly, which is not seen in the observations. Similarly to June 2nd, the observed temperature yields warm anomalies over the Labrador and Greenland. A warm anomaly is also observed in southeastern Europe. The analogue temperature reconstructions can capture the warm anomalies over south Greenland and southeastern Europe and the cool anomalies in the western north Atlantic.

The two examples of high and low correlation scores show that the skill for local temperature reconstructions is not necessarily linked with the global scores. In this geographical choice (80W–35E; 25–70N), a lot of weight is given to the north western Atlantic structure of pressure, because the variance is higher in this region. Reducing the zone of analysis, or providing a heavier weight to Europe in the analogue computation from RMS would improve the local reconstructions, although this requires some trial-and-error that is beyond the scope of the paper.

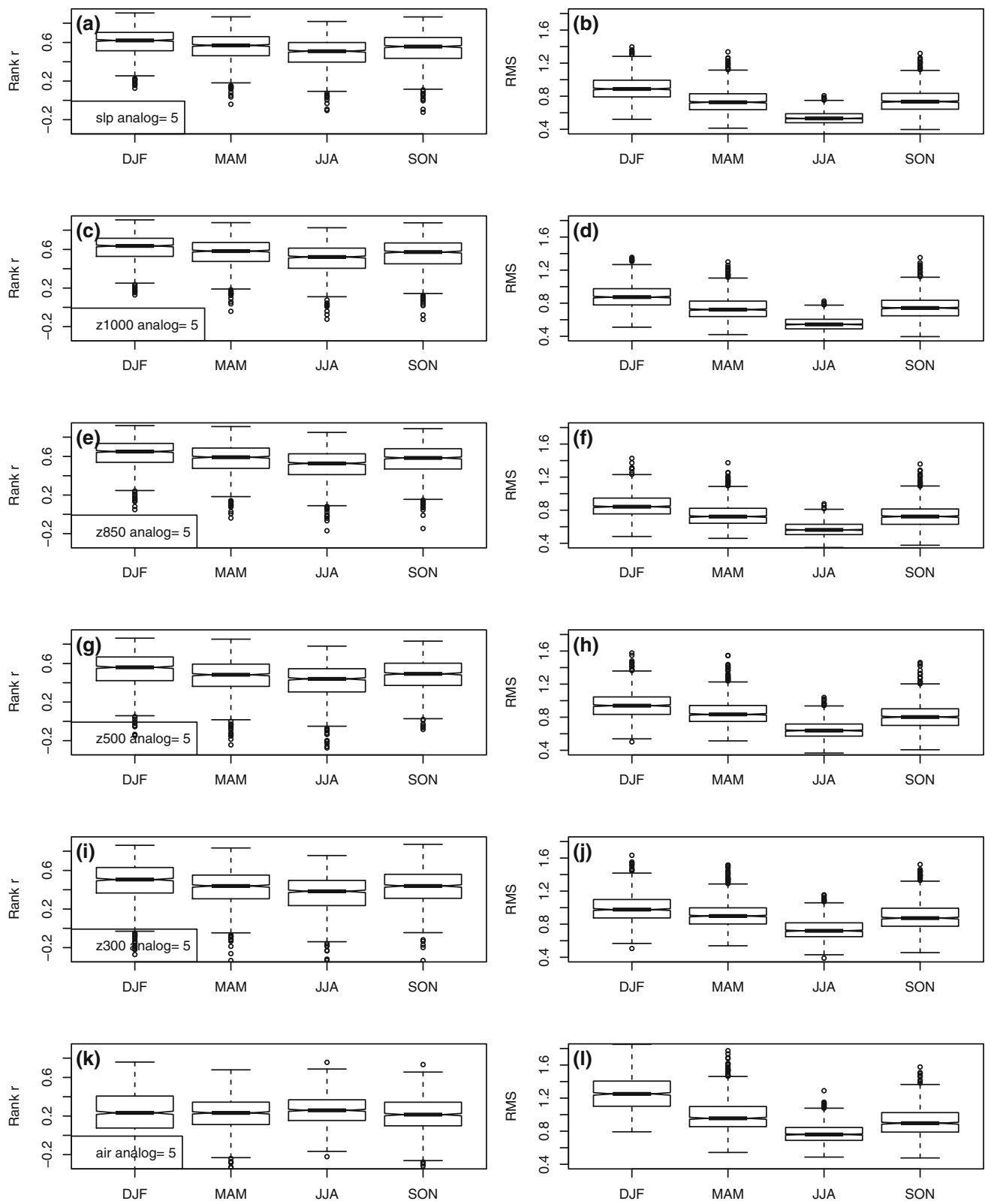
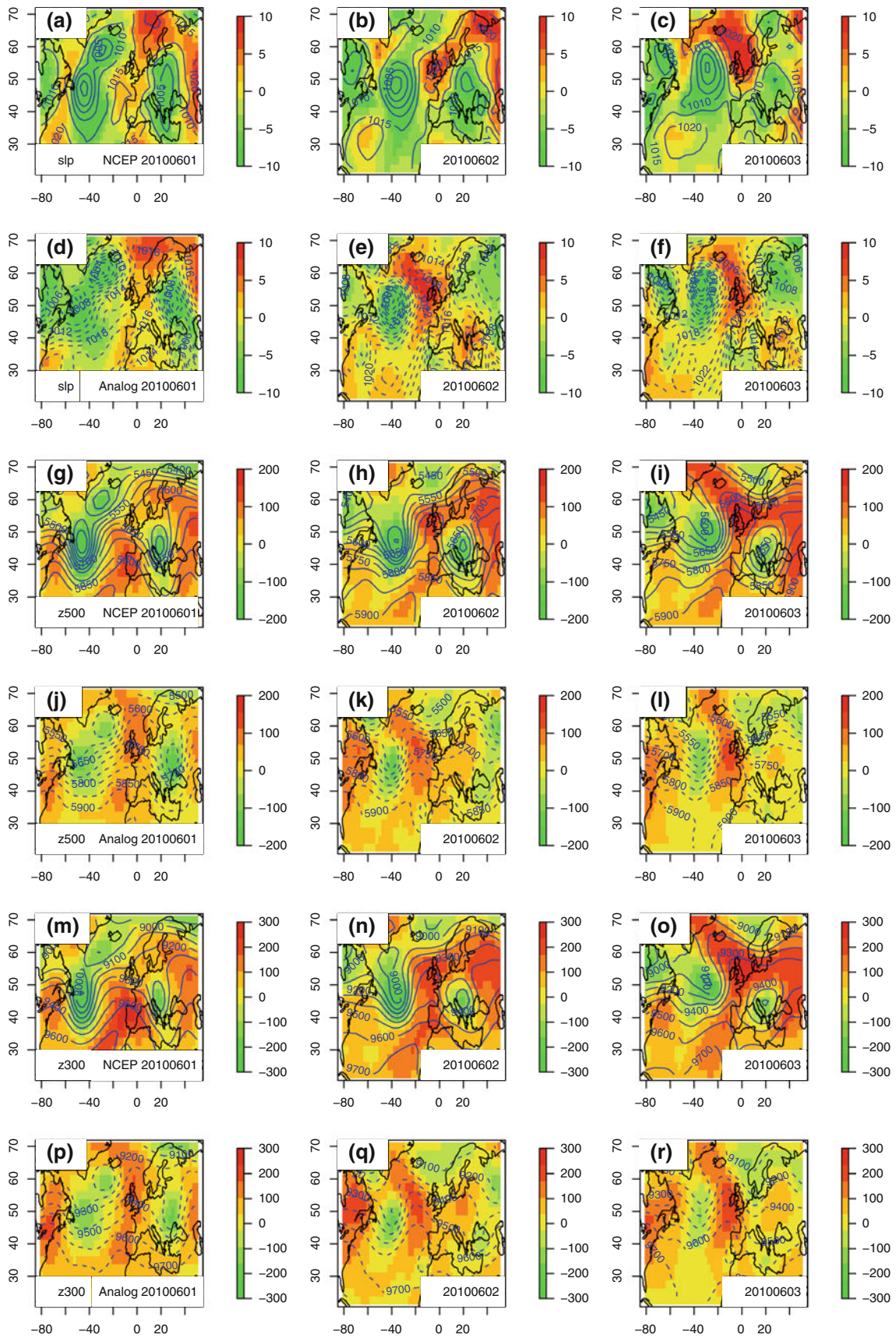


Fig. 5 Seasonality of correlation (*left column*) and RMS (*right column*) values for the first analogue reconstruction of SLP, z1000, z850, z500, z300 and surface air temperature in 2001–2011



◀ **Fig. 6** SLP, z500 and z300 analogue reconstructions for June 1, 2 and 3 2010. *Odd rows* represent NCEP reanalysis fields and *even rows* are for the reconstructions. *Columns* are for the three represented days. The *colors* represent field anomalies (in hPa for SLP, and m for geopotential heights). The *isolines* represent the flow fields (in hPa for SLP, and m for geopotential heights). We use *solid lines* for NCEP reanalysis fields (*odd rows*) and *dashed lines* for reconstructions (*even rows*). Window length is 6 days, time increments $\delta = 3$ days

5 Discussion and conclusion

We have presented a methodology based on analogues to reconstruct an atmospheric field at various pressures, given observations at the surface. This methodology was tested for the 2001–2011 period, for geopotential heights at decreasing pressure levels, from the surface to 300 hPa. We show the results for the year 2010. The differentiability constraint that we imposed results in occasional low correlation scores (which can reach negative values), but the correlation skill is homogeneous for all levels. The differentiability was achieved by considering windows of SLP analogues, which add a constraint to the local direction of the analogue reconstruction. This windowing makes a connection to the embedding theorems that allow a reconstruction of the phase space of an attractor. This theoretical consideration is an attempt to justify the use of windowed analogues to reconstruct the whole atmospheric field. The dimension of the underlying system gives a lower bound on the size of the windows (Haken 1985), which are also limited by the length of the available data.

A more thorough investigation on embedding theory with partial differential equations will be required to achieve a proper mathematical framework.

The coincidence of high and low correlation scores between the reconstruction of sea-level pressure, geopotential heights and surface temperature is not surprising. In the hydrostatic approximation of an air column, geopotential height is linearly related to surface pressure, and sea-level pressure is deduced from surface pressure, altitude and surface temperature. Thus, those variables are naturally correlated: when the reconstruction of SLP is poor, it can be expected that it will be worse for geopotential heights and temperature. And when it is fair, then the probability of higher scores for geopotential height and temperature increases.

We optimized the analogues for the RMS scores giving equal weights to all gridpoints. We found that the first $K = 10$ analogues yield comparable correlation scores (with little loss of RMS scores with respect to the first one). This provides a natural way of generating an ensemble of reconstructions that are consistent with surface conditions, by picking random analogues. For example, if one wants to make a three dimensional reconstruction of atmospheric fields, given daily surface observations from past data, it is possible to propose an ensemble of results that sample the atmospheric variability, especially on the vertical.

This methodology is a low-cost alternative to building a reanalysis by running a climate model assimilating surface observations. The specificity of our approach is that it

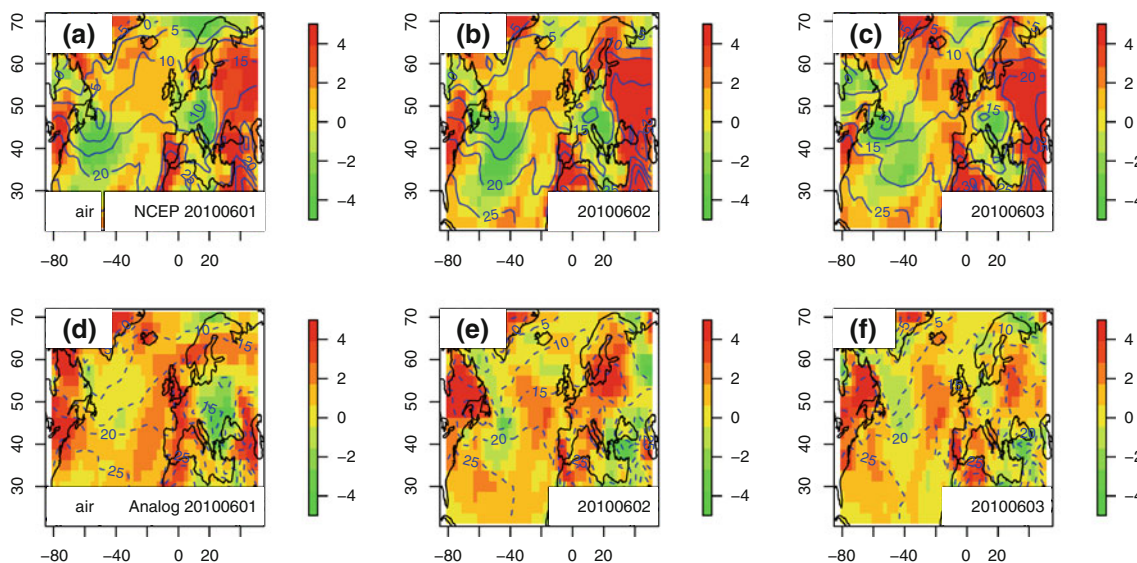
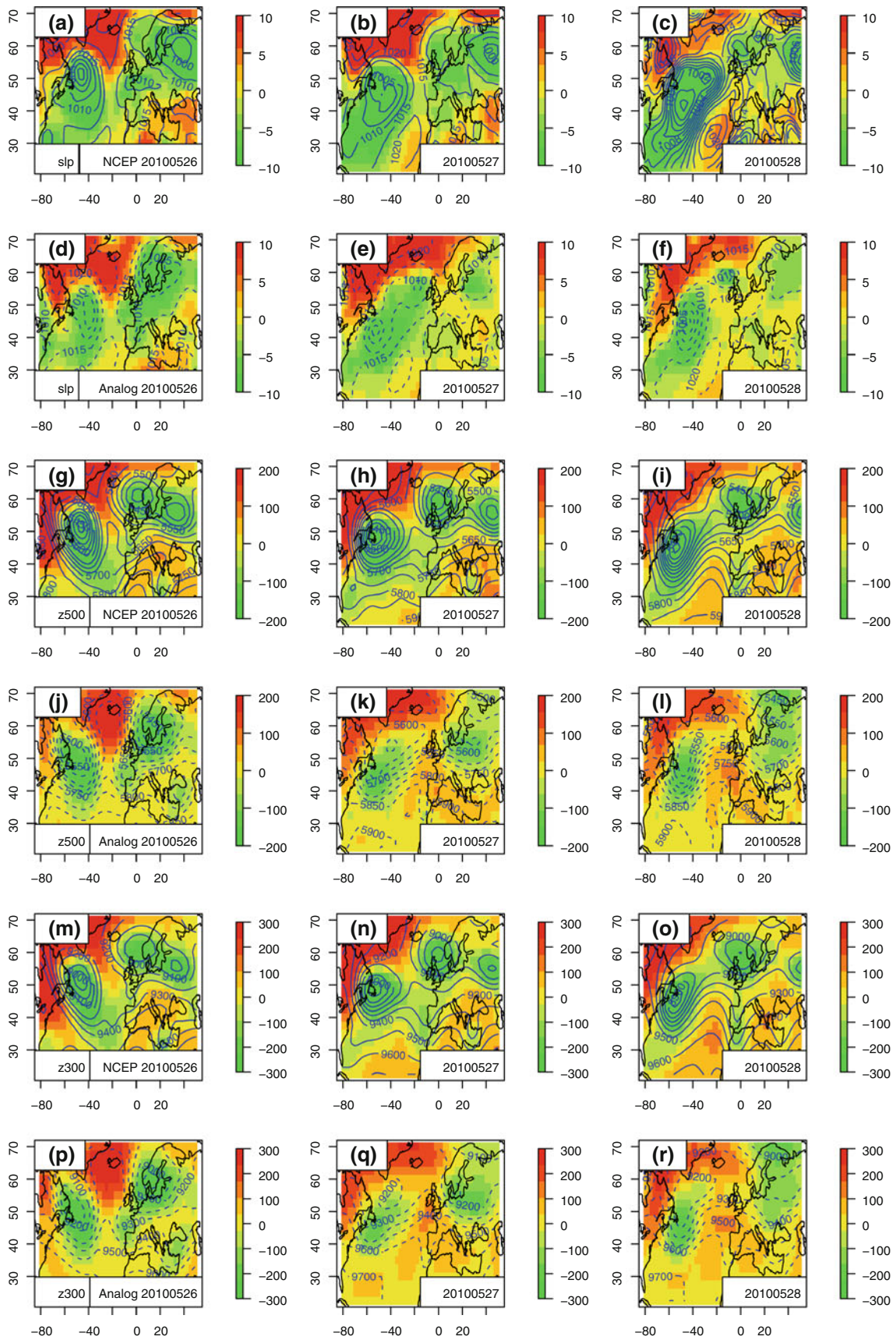


Fig. 7 Surface air temperature analogue reconstructions for June 1, 2 and 3 2010. *Odd rows* represent NCEP reanalysis fields and *even rows* are for the reconstructions. *Columns* are for the three represented days. The *colors* represent temperature anomalies with respect to

seasonal mean (in C). *Isolines* represent the temperature field (in C). We use *solid lines* for NCEP reanalysis fields (*odd rows*) and *dashed lines* for reconstructions (*even rows*). Window length is 6 days, time increments $\delta = 3$ days



◀ **Fig. 8** SLP, z500 and z300 analogue reconstructions for May 26, 27 and 28 2010. *Odd rows* represent NCEP reanalysis fields and *even rows* are for the reconstructions. *Columns* are for the three represented days. We use *solid lines* for NCEP reanalysis fields (*odd rows*) and *dashed lines* for reconstructions (*even rows*). Window length is 6 days, timeshift $\delta = 3$ days

focuses on a region (here the North Atlantic) rather than the globe. We emphasize that its use over a much larger region would probably not give satisfactory results, because the larger the domain, the more difficult it is to obtain suitable analogues of circulation (Lorenz 1969). Yiou et al. (2007) have tested the sensitivity of the results of the analogue scores by shifting the regions of analysis around the North Atlantic and found no significant effect. Schenk and Zorita (2012) have used a similar analogue approach, albeit without the time continuity constraint to make climate inferences in Northern Europe.

From a visual inspection of two cases of high and low scores of the reconstruction (in terms of spatial correlation) it appears that regional behavior is not necessarily connected to global correlations. This does not contradict the findings of Yiou et al. (2007) or Vautard and Yiou (2009) who investigated analogues of temperature for continental Europe only. In order to obtain better scores of pressure or temperature for the North Atlantic basin, it might be desirable to give more weight to the eastern part of the North Atlantic (and less weight to high latitudes) in the distance to be optimized when computing the analogues.

The refinements in the definition of the distance hence need to be evaluated from a priori information on the spatio-temporal variability of the field \mathbf{X} on which the analogues are computed.

The method was tested in a very restricted context with one general dataset [NCEP reanalysis (Kalnay et al. 1996)]. Our formalism allows one to use a long control simulation (e.g. 1,000 years) of a coupled climate model, hence sampling a large part of climate variability as a reference set \mathcal{R} . Such a reference set (a climate model simulation) ensures a consistence between all atmospheric fields at any moment. As we mentioned, the target set \mathcal{T} can stem from observations over a region, in a gridded format. The only constraint is that the sets \mathcal{R} and \mathcal{T} are formulated on the same spatial grid so that correlation and RMS scores can be determined.

We conclude that we have presented a versatile method for generating atmospheric flows constrained by surface observations by exploiting simulations of a climate model. The main caveat is that the reconstructed flow stems from already observed (or simulated) flow and that it is not possible to generate situations that have never been observed. Another caveat is that analogues poorly detect long term trends (Vautard and Yiou 2009) of variables like temperature or precipitation. Therefore, an a priori knowledge of the baseline value of fields like temperature is needed to make reconstructions for remote times, when the climatology (i.e. a reference average) is different.

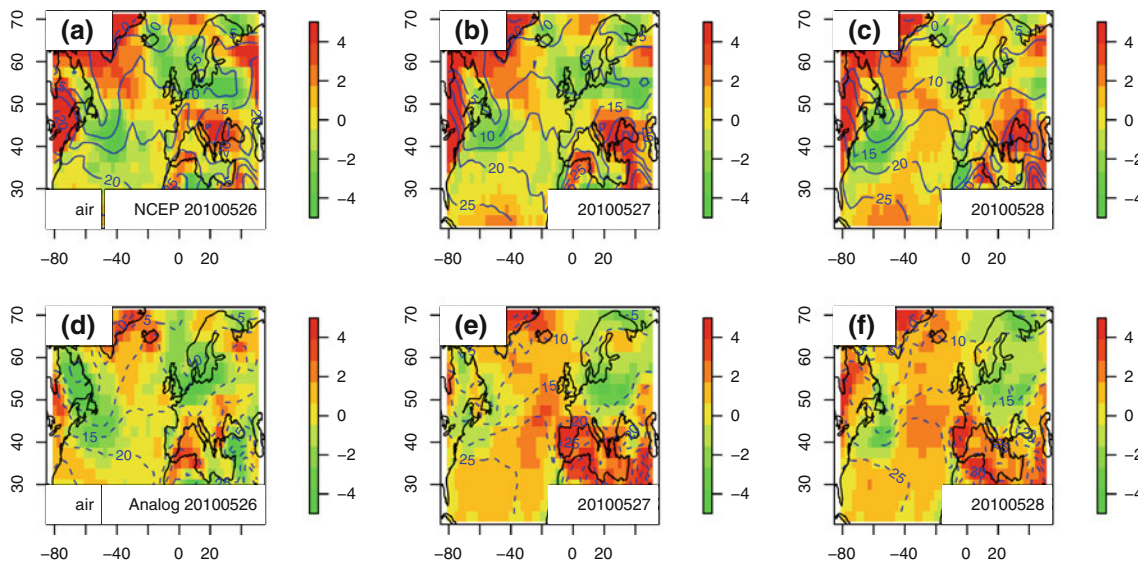


Fig. 9 Surface air temperature analogue reconstructions for May 26, 27 and 28 2010. *Odd rows* represent NCEP reanalysis fields and *even rows* are for the reconstructions. *Columns* are for the three represented

days. We use *solid lines* for NCEP reanalysis fields (*odd rows*) and *dashed lines* for reconstructions (*even rows*). Window length is 6 days, timeshift $\delta = 3$ days

Acknowledgments This work was supported by the French ANR CHEDAR project. PY acknowledges the hospitality of AORI (University of Tokyo), which helped developing some of the ideas of the manuscript. All computations were done with the R language. We thank the two anonymous reviewers for their constructive comments that helped to improve significantly the manuscript.

References

- Ansell T, Jones P, Allan R, Lister D, Parker D, Brunet M, Moberg A, Jacobeit J, Brohan P, Rayner N, Aguilar E, Alexandersson H, Barriendos M, Brandsma T, Cox N, Della-Marta P, Drebs A, Founda D, Gerstengarbe F, Hickey K, Jonsson T, Luterbacher J, Nordli O, Oesterle H, Petrakis M, Philipp A, Rodwell M, Saladie O, Sigro J, Slonosky V, Srnec L, Swail V, Garcia-Suarez A, Tuomenvirta H, Wang X, Wanner H, Werner P, Wheeler D, Xoplaki E (2006) Daily mean sea level pressure reconstructions for the European-north Atlantic region for the period 1850–2003. *J Clim* 19(12):2717–2742
- Cattiaux J, Vautard R, Cassou C, Yiou P, Masson-Delmotte V, Codron F (2010) Winter 2010 in Europe: a cold extreme in a warming climate. *Geophys Res Lett* 37:L20704. doi:[10.1029/2010GL044613](https://doi.org/10.1029/2010GL044613)
- Chenet al, Fluteau F, Courtillot V (2005) Modelling massive sulphate aerosol pollution, following the large 1783 Laki basaltic eruption. *Earth Planet Sci Lett* 236(3–4):721–731
- Compo G, Whitaker J, Sardeshmukh P, Matsui N, Allan R, Yin X, Gleason B, Vose R, Rutledge G, Bessemoulin P, Brönnimann S, Brunet M, Crouthamel R, Grant A, Groisman P, Jones P, Kruk M, Kruger A, Marshall G, Mauerer M, Mok H, Nordli O, Ross T, Trigo R, Wang X, Woodruff S, Worley S (2011) The twentieth century reanalysis project. *Q J R Meteorol Soc* 137:1–28
- Compo GP, Whitaker JS, Sardeshmukh PD (2006) Feasibility of a 100-year reanalysis using only surface pressure data. *Bull Amer Met Soc* 87(2):175–190
- Fischer EM, Seneviratne SI, Lüthi D, Schär C (2007) Contribution of land-atmosphere coupling to recent European summer heat waves. *Geophys Res Lett* 34:L06707. doi:[10.1029/2006GL029068](https://doi.org/10.1029/2006GL029068)
- Ghil M, Allen M, Dettinger M, Ide K, Kondrashov D, Mann M, Robertson A, Saunders A, Tian Y, Varadi F, Yiou P (2002) Advanced spectral methods for climatic time series. *Rev Geophys* 40(1). doi:[10.1029/2001RG000092](https://doi.org/10.1029/2001RG000092)
- Gong DY, Drange H, Gao YQ (2007) Reconstruction of northern hemisphere 500hpa geopotential heights back to the late 19th century. *Theoret Appl Climato* 190(1–2):83–102
- Haken H (1985) Order in chaos. *Comput Meth Appl Mech Eng* 52(1–3):635–652
- Kalnay E, Kanamitsu M, Kistler R, Collins W, Deaven D, Gandin L, Iredell M, Saha S, White G, Woollen J, Zhu Y, Chelliah M, Ebisuzaki W, Higgins W, Janowiak J, Mo K, Ropelewski C, Wang J, Leetmaa A, Reynolds R, Jenne R, Joseph D (1996) The NCEP/NCAR 40-year reanalysis project. *Bull Am Meteorol Soc* 77(3):437–471
- Kimoto M, Ghil M (1993) Multiple flow regimes in the Northern-hemisphere winter. 1. Methodology and hemispheric regimes. *J Atmos Sci* 50(16):2625–2643
- Kondrashov D, Ide K, Ghil M (2004) Weather regimes and preferred transition paths in a three-level quasigeostrophic model. *J Atmos Sci* 61(5):568–587
- Lorenz EN (1969) Atmospheric predictability as revealed by naturally occurring analogues. *J Atmos Sci* 26(4):636–646
- Luterbacher J, Rickli R, Tinguely C, Xoplaki E, Schupbach E, Dietrich D, Husler J, Ambuhl M, Pfister C, Beeli P, Dietrich U, Dannecker A, Davies T, Jones P, Slonosky V, Ogilvie A, Maheras P, Kolyva-Machera F, Martin-Vide J, Barriendos M, Alcoforado M, Nunes M, Jonsson T, Glaser R, Jacobeit J, Beck C, Philipp A, Beyer U, Kaas E, Schmith T, Barring L, Jonsson P, Racz L, Wanner H (2000) Monthly mean pressure reconstruction for the late maunder minimum period (AD 1675–1715). *Int J Climatol* 20(10):1049–1066
- Mañé R (1981) On the dimension of the compact invariant sets of certain non-linear maps. In: Rand DA, Young L-S (eds) *Dynamical systems and turbulence (Lecture Notes in Mathematics)*, vol 898. Springer, Berlin, pp 230–242
- Michelangeli P, Vautard R, Legras B (1995) Weather regimes: recurrence and quasi-stationarity. *J Atmos Sci* 52(8):1237–1256
- Schenk F, Zorita E (2012) Reconstruction of high resolution atmospheric fields for northern europe using analog-upscaling. *Clim Past Discuss* 8:819–868
- Schmidt A, Ostro B, Carslaw K, Wilsona M, Thordarson T, Manna G, Simmons A (2011) Excess mortality in europe following a future laki-style icelandic eruption. *Proc Nat Acad Sci* 108(38):15710–15715
- Seneviratne SI, Lüthi D, Litschi M, Schaer C (2006) Land-atmosphere coupling and climate change in Europe. *Nature* 443(7108):205–209
- Takens F (1981) Detecting strange attractors in turbulence. In: Rand DA, Young L-S (eds) *Dynamical systems and turbulence (Lecture notes in mathematics)*, vol 898. Springer, Berlin, pp 366–381
- Uppala SM, Kallberg PW, Simmons AJ, Andrae U, Bechtold VD, Fiorino M, Gibson JK, Haseler J, Hernandez A, Kelly GA, Li X, Onogi K, Saarinen S, Sokka N, Allan RP, Andersson E, Arpe K, Balmaseda MA, Beljaars ACM, VanDe Berg L, Bidlot J, Bormann N, Caires S, Chevallier F, Dethof A, Dragosavac M, Fisher M, Fuentes M, Hagemann S, Holm E, Hoskins BJ, Isaksen L, Janssen PAEM, Jenne R, McNally AP, Mahfouf JF, Morcrette JJ, Rayner NA, Saunders RW, Simon P, Sterl A, Trenberth KE, Untch A, Vasiljevic D, Viterbo P, Woollen J (2005) The ERA-40 re-analysis. *Q J R Meteorol Soc* 131(612):2961–3012
- Vautard R, Yiou P (2009) Control of recent European surface climate change by atmospheric flow. *Geophys Res Lett* 36. doi:[10.1029/2009GL040480](https://doi.org/10.1029/2009GL040480)
- Vautard R, Yiou P, Ghil M (1992) Singular-spectrum analysis—a toolkit for short, noisy chaotic signals. *Phys D* 58(1–4):95–126
- Vautard R, Yiou P, D’Andrea F, de Noblet N, Viovy N, Cassou C, Polcher J, Ciais P, Kageyama M, Fan Y (2007) Summertime European heat and drought waves induced by wintertime Mediterranean rainfall deficit. *Geophys Res Lett* 34:L07711. doi:[10.1029/2006GL028001](https://doi.org/10.1029/2006GL028001)
- Widmann M, Goosse H, van der Schrier G, Schnur R, Barkmeijer J (2010) Using data assimilation to study extratropical northern hemisphere climate over the last millennium. *Clim Past* 6(5):627–644
- Yiou P, Vautard R, Naveau P, Cassou C (2007) Inconsistency between atmospheric dynamics and temperatures during the exceptional 2006/2007 fall/winter and recent warming in Europe. *Geophys Res Lett* 34:L21808. doi:[10.1029/2007GL031981](https://doi.org/10.1029/2007GL031981)
- Zampieri M, D’Andrea F, Vautard R, Ciais P, de Noblet-Ducoudré N, Yiou P (2009) Hot European Summers and the role of soil moisture in the propagation of Mediterranean drought. *J Clim* 22:4747–4758
- Zorita E, von Storch H (1999) The analog method as a simple statistical downscaling technique: comparison with more complicated methods. *J Clim* 12:2474–2489